- RESEARCH PAPER -

International Journal of Mining and Geo-Engineering

IJMGE

IJMGE 55-2 (2021) 97-107

DOI: 10.22059/IJMGE.2020.289423.594826

Investigation of the effect of industrial ball mill liner type on their comminution mechanism using DEM

Sajad Kolahi [a], Mohammad Jahani Chegeni [a, *], Kumars Seifpanahi Shabani [a]

[a] *Faculty of Mining, Petroleum & Geophysics Engineering, Shahrood University of Technology, Shahrood, Iran*

Article History:

Received: 22 September 2019,

Revised: 31 October 2019,

Accepted: 21 September 2020.

ABSTRACT

The mill shell liner type, rotation speed and the amount of its loading are the key factors influencing the charging behavior, consequently the comminution mechanism. In this paper, the milling operation of industrial ball mills using the Discrete Element Method (DEM) is investigated. First, an industrial scale ball mill with a Smooth liner type is simulated. Then, by changing liner type, i.e. Wave, Rib, Ship-lap, Lorain, Osborn, and Step liners, six other independent simulations are performed. Effects of mill shell liner type on charge shoulder, toe, impact, and head points, also on head height and impact zone length as well as on the creation of cascading, cataracting, and centrifuging motions for balls at two different mill speeds, i.e. 70% and 80% of its critical speed (N_C) are evaluated. Also, in order to validate simulation results, a laboratory-scale mill is simulated. The results indicate that the charge heads are respectively about 240.13, 283.40, 306.47, 278.12, 274.42, 274.42, and 278.12 cm at the simulations performed with Smooth, Wave, Rib, Ship-lap, Lorain, Osborn, and Step liners at 70% of N_C. The corresponding values at 80% of N_C are as follows: 256.08, 264.56, 313.54, 298.45, 313.54, 311.60, and 283.40 cm. On the other hand, the impact zone lengths are respectively about 33.14, 22.11, 38.63, 35.86, 38.63, 38.63, and 49.59 cm at the simulations performed with the above-mentioned liners at 70% of N_C. The corresponding values for impact zone lengths at 80% of N_C are as follows: 35.86, 27.63, 49.59, 38.63, 33.14, 52.32, and 41.38 cm. Comparison of the simulations related to the laboratory scale mill with experimental results demonstrates a good agreement that validates the DEM simulations and the software used.

Keywords: *DEM simulation, Industrial ball mills, Liner type, Head height, Impact zone length*

1. Introduction

Grinding is the most common process used to liberate valuable minerals from the gangue. Ball mills have been used mainly in the mineral processing industry since the mid of 19th century due to the need for finer material. However, there is still a need for understanding the combined and individual effects of all design and operating variables to make the process more efficient [1]. Mishra and Rajamani [2] were the first ones to track the motion of the ball charge in large-diameter ball mills using DEM simulation. Later, Powell and McBride [3] illustrated the media motion and grinding regions (head, departure shoulder, center of circulation, equilibrium surface, bulk toe, and impact toe). In the last three decades, the importance of lifter on the charging behavior in tumbling mills has been discussed. Cleary [4,5] used DEM to predict the wear of lifters and the power draw of ball mills. Kalala et al. [6,7] investigated the wear of lifter profiles for the mills grinding dry coal. Banisi and Hadizadeh [8] used a mechanical lifter wear monitor to measure the mass loss due to the wear in the SAG mill. Modification of SAG mill liner shape based on 3D liner wear profile measurements was conducted by Yahyaei et al. [9]. Many researchers have been working on simulating the tumbling mills using the DEM method [10–23]. Examples of 3D models of SAG mills were presented along with detailed predictions of power draw, liner wear rates, liner stresses, and energy spectra by Cleary [10]. Abd El-Rahman et al. indicated that DEM successfully predicts power draft in a variety of semi-autogenous plant operations [11]. Predictions of flow patterns in a 600-mm scale model SAG mill were made using four classes of discrete element method (DEM) models and were compared to experimental photographs by Cleary et al. [12]. A review of computer simulation of tumbling mills by the discrete element method was conducted by Mishra [13] where practical applications of DEM were studied. Various ways of extracting collision data from the DEM model and translating it into breakage estimates were described by Morrison and Cleary [14] where the different breakage mechanisms (impact and abrasion) and the specific impact histories of the particles in order to assess the breakage rates for various size fractions in the mills were investigated. The discrete element method was used by Djordjevic et al. [15] to model the effects of lifter height (5–25cm) and mill speed (50–90% of critical) on the power draw and frequency distribution of specific energy (J/kg) of normal impacts in a 5m diameter autogenous (AG) mill. Also, comminution patterns within a pilot-scale AG/SAG mill were modeled by Djordjevic et al. [16]. By gradually increasing the tumbling model SAG mill length and analyzing the charge trajectory and shape variation at given operating conditions (i.e., ball filling, mill speed, liner type), the impact of the end-wall effect on the charge trajectory in model mills was investigated by Maleki-Moghaddam et al. [17]. A relationship between charge shape characteristics and fill level and lifter height for a SAG mill was obtained by Owen and Cleary [18]. Estimating energy in grinding using DEM modeling was conducted by Weerasekara et al. [19] where they explored the breakage environment in mills using DEM techniques, and how these techniques may be expanded to provide more useful data for mill and comminution device modeling. A campaign of DEM simulations was performed by varying the mill size and charge particle size distribution to explore and understand the breakage environment in mills using DEM techniques [19]. Analysis of each mill

* Corresponding author. *E-mail address:* m.jahani1983@gmail.com (M. Jahani Chegeni).

was conducted through consideration of the total energy dissipation and the nature of the collision environment that leads to comminution [19]. Development of models relating charge shape and power draw to SAG mill operating parameters and their use in devising mill operating strategies to account for liner wear was conducted by Cleary and Owen [20]. Numerical prediction of wear in SAG mills based on DEM simulations was performed by Xu et al. [21] where the 3D simulations were performed using DEM combined with an erosion model, which is referred to as Shear Impact Energy Model (SIEM), to predict wear within a SAG mill. The effect of operating condition changes on the collisional environment in a SAG mill was investigated by Cleary and Owen [22]. The role of end liners in dry SAG mills to obtain a thorough understanding of the effects of end liners design on the load trajectory and SAG mill performance was experimentally studied by Hasankhoei et al. [23]. The test works were conducted in a scale-down mill with a diameter of 1 m. It was shown that the liner in the first and the last 20% of the mill length which were under the protection of the deflector liners experienced no deformation [23].

Grinding consumes most of the energy in mineral processing. Ball mill is an important kind of grinding equipment used to decrease the size of ore particles. The power consumption of a ball mill is one of the most important parameters to consider in the design of a ball mill because it determines its economic efficiency. The power consumption is usually determined by charge fill level, lifter height, lifter number, and mill speed. However, almost all of the classical theories for calculating the power consumption of ball mills disregard the effect of lifters and only focus on rotation rate, charge fill level, as well as size and shape of grinding media, thereby may causing errors [24]. Mill liners protect mill shells from abrasion and lift ore particles and grinding media to a high position. Therefore, liners/lifters must be able to bear high-impact loads during the grinding process. The wear rate of these components is high, and these parts tend to break or incur wear-out failure, which can seriously affect the production efficiency of ball mills. Thus, the research on the liner structure and configuration of ball mills is crucial to improve the production ability and economy of ball mills [24].

The mineral processing industry could save about 70% of the power involved in grinding processes if this power were reduced to its practical minimum power consumption [25]. In this context, achieving a more efficient grinding in ball mills is an important issue, since they have a low-efficiency rate partially due to lack of creation of cascading and cataracting motions for balls and inappropriate shoulder and toe points [26]. For a given amount of balls, if the mill rotation speed is higher than or equal to its critical speed, the balls stick to the mill wall and the grinding operation does not happen, and centrifuging movements are created. On the other hand, if the mill speed is between 80 to 100% of its critical speed, the suitable shoulder and toe points are not created and the grinding energy is used to hit the balls with the mill wall, in this mode centrifuging movements may also be created. However, if the mill speed is between 60% and 80% of its critical speed, the appropriate shoulder and toes point as well as cascading and cataracting movements are created which results in better grinding. In this case, the dominant mechanism will be impacted, which is the optimum mode for the process and will reduce the power consumption of the mill. Meanwhile, the abrasion mechanism is not very effective in this mode. At speeds less than 60% of critical speed, cascading and cataracting movements gradually disappear and the balls roll over each other. In this case, grinding is not optimal and the abrasion mechanism plays a more effective role [26]. Among other effective factors in creating cascading and cataracting movements in mills, lifters can be mentioned. Lifters cause the balls to climb to a higher elevation and prevent their slipping [26].

Simulation has become a common tool in the design and optimization of industrial processes [27–29]. The continuous increase in computing power is now enabling researchers to implement numerical methods that do not focus on the granular assembly as an entity, but rather deduce its global characteristics from observing the individual behavior of each particle [30]. Due to their highly discontinuous nature, one should expect that granular media require a discontinuous simulation method. Indeed, to date, the Discrete Element Method (DEM) is the leading approach to those problems [30]. Because of its inherent advantages in analyzing granular materials, DEM has been developed rapidly in recent decades and is used widely in mineral processing engineering [31–33].

To control, optimize, and reduce ball mill power consumption, mineral processing engineers must obtain enough information about their operation conditions. One of the most effective techniques is the use of computer simulations. Computer simulations using methods such as DEM can be effective to find the optimal speed of ball mills and as a result, creating appropriate shoulder and toe points in them as well as creating cascading and cataracting motions. This method can also be used to prevent centrifugal movements. In this research, DEM is introduced and used, utilizing an open-source software LIGGGHTS, to simulate the milling operation of the industrial scale ball mills. An industrial-scale ball mill with a Smooth liner type is simulated. Then, by changing liner type, i.e. Wave, Rib, Ship-lap, Lorain, Osborn, and Step liners, six other independent simulations are performed. Also, in this paper, it has been shown that shoulder height and toe height are not suitable criteria for investigating impact mechanisms and improving mill performance. For this purpose, two new parameters, called 'head height' and 'impact zone length', are introduced instead of them. The charge head height means the highest altitude when the particles begin to detach from the mill and begin their cataracting motion. Also, the impact zone length is the difference in the length of the toe point with the highest endpoint of the cataract motion (impact point) (Figure 1). Additionally, effects of mill shell liner type on charge shoulder, toe, impact, and head points, also on head height and impact zone length as well as on the creation of cascading, cataracting, and centrifuging motions for balls at two different mill speeds, i.e. 70% and 80% of its critical speed (N_C) are evaluated. Also, in order to validate simulation results, a laboratory-scale mill is simulated. In this research, for the first time, the effect of different mill liner types on two new parameters introduced by the authors i.e. 'head height' and 'impact zone length' and as a result on impact mechanism and performance of industrial-scale ball mills at different mill speeds (70% and 80% of critical speed) using discrete element method are investigated.

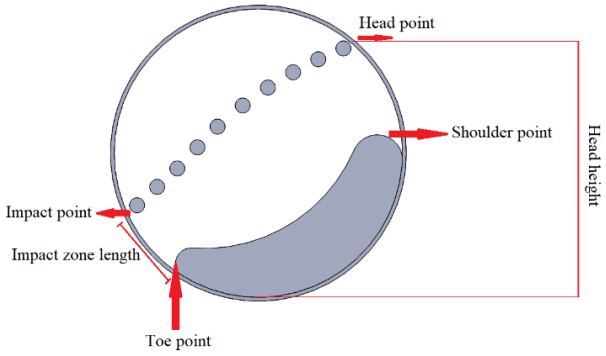

Figure 1. Charge head, shoulder, toe, and impact points as well as head height and impact zone length

2. Simulation Method

2.1. The DEM method to predict particle flow

The Discrete Element Method is a numerical technique used to predict the behavior of collision-dominated particle flows. Each particle in the flow is tracked and all collisions between particles and between particles and boundaries are modeled. The Discrete Element Method is a powerful numerical tool for simulating the mechanical behavior of systems with a large number of particles based on particles' motion and interactions and their representation as rigid geometric bodies, commonly having spherical shape [34,35]. Whereas simulations with spherical particles can include millions of particles, using non-spherical particles is still not an easy task. Whereas for spherical particles the geometry is described by the radius and the interaction forces can easily be calculated by contact laws like Hertzian contact, for non-spherical

particles the geometry representation and calculation of contact forces are much more complex [34,36]. DEM is based on the Lagrangian approach and treats granular material as an assemblage of distinct particles, each governed by physical laws [37,38]. Each particle interacts with its neighbors through particle-to-particle contacts which can be formed or broken at each time step [35,37,39–41]. In recent years, the drastic increase in affordable computational power has allowed DEM simulations to become a versatile tool for industrial applications [42]. Recent advances in discrete element modeling have resulted in this method becoming a useful simulation tool that can provide detailed information not easily measured during experiments [43]. With the maturing of DEM simulation, it is now becoming possible to run simulations of millions of particles with complex shapes and inter-particle cohesive forces intolerable times on single processor, desktop computers [27,42–44].

In this research, an open-source software LIGGGHTS was used to perform DEM simulations. The DEM variant used here is sometimes called a 'soft particle method'. The particles are allowed to overlap and the extent of overlap is used in conjunction with a contact force law to give instantaneous forces from knowledge of the current positions, orientations, velocities, and spins of the particles [45]. Here we have used Hertz–Mindlin's contact force law. It states that the repulsive force resulting from a collision is calculated from the amount of normal overlap δ_n and tangential overlap δ_t (soft-sphere approach) [46]. This granular model uses the following formula for the frictional force between two granular particles, when the distance r between two particles of radii R_i and R_j is less than their contact distance $d = R_i + R_j$. There is no force between the particles when $r > d$:

$$\mathbf{F} = \left(k_n \boldsymbol{\delta n_{ij}} - \gamma_n \mathbf{vn_{ij}}\right) + \left(k_t \boldsymbol{\delta t_{ij}} - \gamma_t \mathbf{vt_{ij}}\right) \quad (1)$$

The first term is the normal force ($\mathbf{F_n}$) between the two particles and the second term is the tangential force ($\mathbf{F_t}$). The normal force has two terms: a spring force and a damping force. The tangential force also has two terms: a shear force and a damping force. The sheer force is a "history" effect that accounts for the tangential displacement (tangential overlap) between the particles for the duration of the time they are in contact.

The quantities in the equation are as follows:

k_n: elastic constant for normal contact

$\boldsymbol{\delta n_{ij}}$: d − r = normal overlap (overlap distance between the two particles)

γ_n: viscoelastic damping constant for normal contact

$\mathbf{vn_{ij}}$: normal relative velocity (a normal component of the relative velocity of the two particles)

k_t: elastic constant for tangential contact

$\boldsymbol{\delta t_{ij}}$: tangential overlap (tangential displacement vector between the two spherical particles which is truncated to satisfy a frictional yield criterion)

γ_t: viscoelastic damping constant for tangential contact

$\mathbf{vt_{ij}}$: tangential relative velocity (a tangential component of the relative velocity of the two particles).

Considering that the shear modulus (G) can be calculated from Young's modulus and Poisson ratio, the Hertz–Mindlin contact model depends on the following material parameters [46]:

Coefficient of restitution, e

Young's modulus, Y

Poisson ratio, ν

Coefficient of static friction, μ_s

Coefficient of rolling friction, μ_r.

The maximum overlap between particles is determined by the stiffness k_n of the spring in the normal direction. Typically, average overlaps of 0.1–0.5% are desirable, requiring spring constants of the order of 10^4–10^6 N/m in three dimensions. The normal damping coefficient γ_n is chosen to give the required coefficient of restitution e (defined as the ratio of the post-collisional to the pre-collisional normal component of the relative velocity) [47].

In DEM, particles are traditionally approximated by disks or spheres, in two and three dimensions, respectively. These shapes are preferred because of their computational efficiency. The contact is always on the line joining the center of each particle and is as simple as comparing the distance between their centers to the sum of their radii [42,44]. Since in SAG mills, balls are spherical, DEM can be appropriately used to simulate their motion.

The drawback of the DEM method is that the time step has to be chosen extremely small because the contact force exhibits a very stiff behavior. Depending on the material properties and the particle size the time step size can be as low as 10^{-6} s for an accurate simulation [48 – 50].

3. Ball Mill Configuration

In this work, an industrial scale ball mill with a Smooth liner type is simulated. Then, by changing liner type, i.e. Wave, Rib, Ship-lap, Lorain, Osborn, and Step liners, six other independent simulations were performed (Fig. 2). It is worth noting that liner types used in this study were selected based on the dimensions available in Figure 7.11 of the B. A. Wills' book [51] and drawn using reverse engineering.

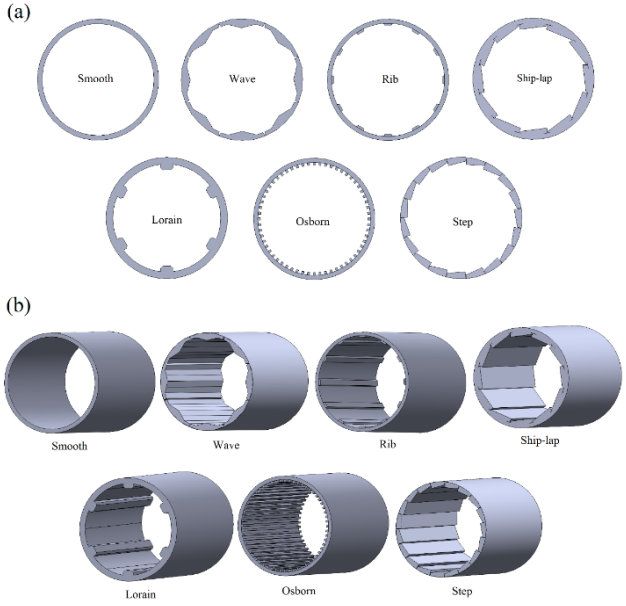

Figure 2. 2D (a) and 3D (b) geometries of industrial ball mills with different liner types: Smooth, Wave, Rib, Ship-lap, Lorain, Osborn, and Step.

The detailed geometrical, operational conditions, material properties, and calculations for these industrial-scale ball mills are listed in Tables 1 – 4. It should be noted that the material of the balls used in the simulations is stainless steel. Parameters that are used in Table 4 such as ball density, the ball sliding friction coefficient, ball rolling friction coefficient, Poisons ratio, Young's modulus, and ball restitution coefficient are belonging to stainless steel and are obtained from the internet. It is worth noting that in this research all balls have the same diameter of 6 cm. The reason for keeping the ball diameter constant is to prevent the effect of changing their size on the charge head height and impact zone length. Optimizing the ball size distribution for all liners used in this study is the subject of the authors' future researches.

4. Results and Discussion

Fig. 3 demonstrates snapshots of 2D and 3D of the simulations of the industrial ball mills with different liner types: Smooth, Wave, Rib, Ship-lap, Lorain, Osborn, and Step when the drum was rotating at 70% of its critical speed using the DEM method, respectively. Also, Fig. 4 demonstrates snapshots of 2D and 3D simulations of the industrial ball

mills with the above-mentioned liner types when the drum was rotating at 80% of its critical speed.

Table 1- Industrial ball mill dimensions.

Industrial-scale ball mill	Dimensions
Smooth mill shell thickness (cm)	13.5
Mill length (m)	5.70
Mill diameter (m)	3.17
Mill volume at Smooth mode (m^3)	44.9866
N_C (Critical speed) (rpm)	23.99
Rotation speed (70% of N_C) (rpm)	16.79
Rotation speed (80% of N_C) (rpm)	19.19
The direction of rotation of the mill	Counter-clockwise
Maximum thickness of Wave liner (cm)	24.38
Maximum thickness of Rib liner (cm)	17.88
Maximum thickness of Ship-lap liner (cm)	27.27
Maximum thickness of Lorain liner (cm)	36.16
Maximum thickness of Osborn liner (cm)	20.15
Maximum thickness of Step liner (cm)	22.72

Table 2- DEM ball Size distribution and Specification

Ball size class (mm)	Mass fraction (%)
60	100

Table 3- DEM ball Specifications and calculations.

Ball diameter (mm)	60
Ball radius (mm)	30
The volume of one ball (m^3)	1.13×10^{-4}
Volume of all balls (m^3)	20% × 44.9866 = 8.9973
# Balls	$8.9973/1.13 \times 10^{-4} = 79553$
Total mass of balls (kg)	8050 × 8.9973 = 72428.44
Mass rate (kg)	7242.84 (10 steps)
Period of 70% N_C	60/16.79 = 3.5735
Period of 80% N_C	60/19.19 = 3.1268
Neighbor (Particle interaction distance) (m)	$5\% \times 30$ mm = 15×10^{-4}

Table 4- Parameters used for the DEM simulations of pilot scale ball mill.

DEM model details	Value
% Fill of ball charge	40%
# DEM balls in simulation	79553
The total mass of ball charge (kg)	72428.44
DEM spring constant (kg/m)	10^6
Ball density (kg/m^3)	8050
Ball sliding friction coefficient	0.5
Ball rolling friction coefficient	0.0015
Poisons ratio	0.285
Young's modulus (N/m^2)	1×10^9
Ball restitution coefficient	0.817

The following results are obtained from Fig. 3: In Smooth, Wave, and Step liners, due to their appearance, the head height is not created properly and the balls slide over each other. As a result, the abrasion mechanism on these liners is more than other liners. But in edged and angled liners such as Rib, Ship-lap, Lorain, and Osborn the appropriate head height is created. Another important issue with these liners is the number of lifters and their thickness. For example, the Lorain liner, which has 6 thick lifters, provides the proper head height, but because of the low number of lifters, the impact zone length is not created properly in it. However, in the Rib liner, which has 12 low-thickness lifters, due to enough number of lifters, both head height and impact zone length is properly created. On the other hand, in the Osborn liner, increasing the number of lifters to 60 causes balls to be trapped between the lifters, due to the equal distance between the lifters and the diameter of the selected balls (6 cm) in this study. In this liner, the presence of a large number of lifters causes a significant percentage of the balls to stick to the mill wall and causes centrifugal motion, so most of the balls will not participate in the comminution mechanism. Also, by changing the size distribution of the balls, their trapping rate may change, which will be investigated in future researches by the authors. It should be noted that the Osborn liner has both a good head height and a good impact zone length. In the Ship-lap liner, due to its sharp or acute angle, a small portion of the balls adhere to the mill wall and do not participate in comminution operation.

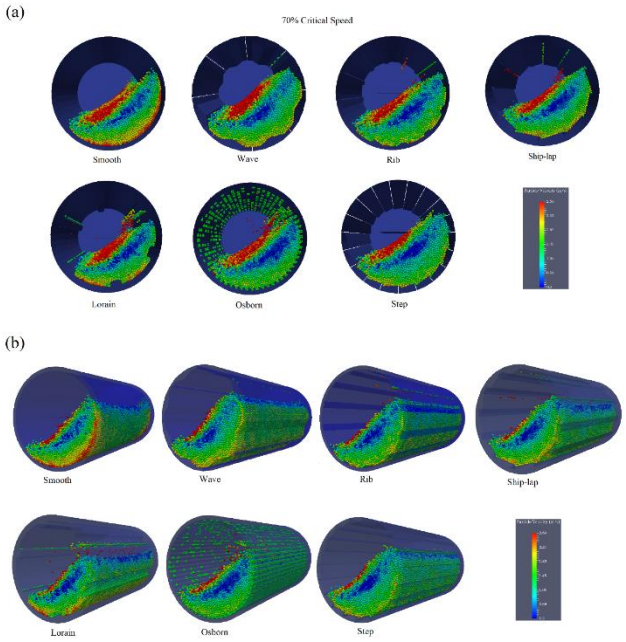

Figure 3. 2D (a) and 3D (b) snapshots showing the motion of particles on the industrial ball mill with different liner types: Smooth, Wave, Rib, Ship-lap, Lorain, Osborn, and Step when the drum was rotating at 70% of its critical speed using DEM method.

The following results are obtained from Fig. 4: In this Figure, it is attempted to improve the performance of the liners by increasing the mill rotation speed by 10%, but this does not have a significant effect on the impact mechanism improvement in most mills. Increasing the mill speed has significantly increased the charge head height on the Lorain and Osborn liners, but has not eliminated the problem of the low or high number of lifters in them. It is worth noting that at Osborn liner, as the mill speed increases, there is no change in the number of balls attached to the mill wall because the main cause of the balls being trapped is a large number of lifters and the equal distance between the lifters and the ball diameter. According to Figures 3 and 4, as well as research conducted and ongoing by the authors of this paper, the optimum number of lifters for ball mills is between 8 and 32 lifters with a medium thickness. Wave, Rib, and Ship-lap liners have an appropriate number of lifters but the number of Lorain liner lifters is less than optimal. Therefore, it is suggested to improve its performance dramatically by increasing the number of lifters to 8 to 12 (due to their high thickness). But in the Osborn liner, because of the excessive number of lifters, it is suggested to reduce the number of lifters to 16 to 32 (due to their low thickness) to improve the performance of the liner. It is worth noting that optimizing the performance of each of these liners will be the subject of future research by the authors of this article. Also, in the Ship-lap and Step liners, by increasing the acute angle and removing the corners in their lifters, the balls can be prevented from adhering to the mill wall.

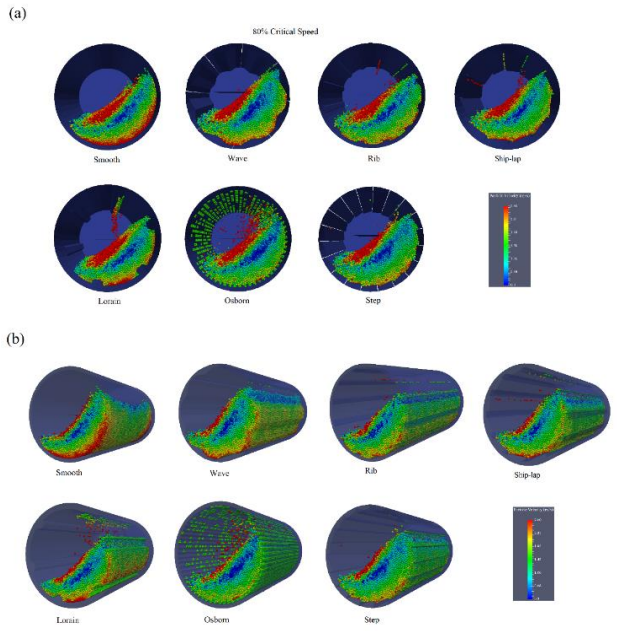

Figure 4. 2D (a) and 3D (b) snapshots showing the motion of particles on the industrial ball mill with different liner types: Smooth, Wave, Rib, Ship-lap, Lorain, Osborn, and Step when the drum was rotating at 80% of its critical speed using DEM method.

Fig. 5 demonstrates how to measure the angle of the charging shoulder, toe, impact, and head points (degree) as well as head height (cm) and impact zone length (cm) using an online protractor in the industrial ball mills with different liner types: Smooth, Wave, Rib, Ship-lap, Lorain, Osborn, and Step, respectively when the drum was rotating at 70% (a) and 80% (b) of its critical speed using DEM method.

The exact values of the height (cm) and angle (degree) of the shoulder, toe, and head points as well as impact zone length (cm) of the balls for the industrial ball mills with the above-mentioned liner types at different drum speeds, are available in Table 5.

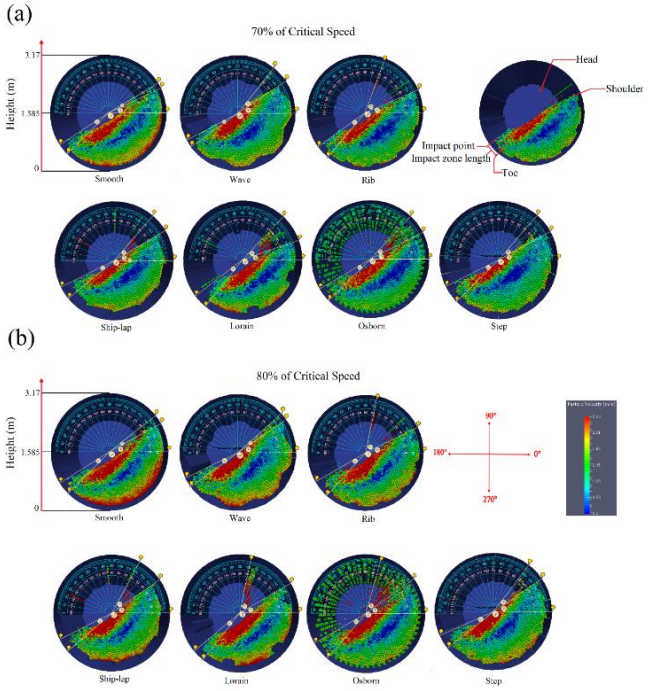

Figure 5. Using an online protractor to determine the height (cm) and angle (degree) of the shoulder, toe, and head points as well as impact zone length (cm) in the industrial ball mills with different liner types: Smooth, Wave, Rib, Ship-lap, Lorain, Osborn, and Step when the drum was rotating at 70% (a) and 80% (b) of its critical speed using DEM method.

Table 5 - Values of the height and angle of the shoulder, toe, and head points as well as impact zone length of the balls for the industrial ball mills with different liner types: Smooth, Wave, Rib, Ship-lap, Lorain, Osborn, and Step at different drum speeds.

Mill liner type	Critical speed (%)	Cascade motion	Cataract motion	Centrifuge motion	Head height (cm)	Shoulder height (cm)	Toe height (cm)	Impact zone length (cm)	Head angle (degree)	Shoulder angle (degree)	Toe angle (degree)	Impact zone angle (degree)
Smooth	70	yes	no	no	**240.13**	225.48	46.42	**33.14**	31	25	225	213
Wave	70	yes	yes	no	**283.40**	247.13	65.34	**22.11**	52	34	216	208
Rib	70	yes	yes	no	**306.47**	220.43	38.88	**38.63**	69	23	229	215
Ship-lap	70	yes	yes	yes	**278.12**	237.75	56.62	**35.89**	49	30	220	207
Lorain	70	yes	yes	yes	**274.42**	210.10	33.60	**38.63**	47	19	232	218
Osborn	70	yes	yes	yes	**274.42**	230.46	46.42	**38.63**	47	27	225	211
Step	70	yes	yes	no	**278.12**	235.34	46.42	**49.59**	49	29	225	207
Smooth	80	yes	no	no	**256.08**	235.34	46.42	**35.89**	38	29	225	212
Wave	80	yes	no	no	**264.56**	247.13	65.34	**27.62**	42	34	216	206
Rib	80	yes	yes	no	**313.54**	227.98	42.58	**49.59**	78	26	227	209
Ship-lap	80	yes	yes	yes	**298.45**	249.41	54.51	**38.62**	62	35	221	207
Lorain	80	yes	yes	no	**313.54**	237.75	35.32	**33.14**	78	30	231	219
Osborn	80	yes	yes	yes	**311.60**	251.66	37.08	**52.32**	75	36	230	211
Step	80	yes	yes	yes	**283.40**	247.13	60.92	**41.38**	52	34	218	203

At first glance, the results of Figure 5 and Table 5 may seem simple software outputs from DEM. However, after simulations, all the required information is available on the motion of all individual particles. So that the researcher (mineral processing engineer) can examine the position of each particle and its movement, which leads to the identification of charge head height and impact zone length, which is the main purpose of this study.

Figure 5 and Table 5 show the following results: There is a cascade motion in all the liners. There is no cataracting motion in the Smooth liner. Also, only in the Wave liner, with the increase of the mill speed, the cataract motion disappears, indicating that increasing the mill speed has an adverse effect on its performance. At 70% of critical speed, centrifugal motion is observed in Ship-lap, Lorain, and Osborn liners, which is much more dramatic in the Osborn liner according to the above-mentioned reasons. Also, at 80% of critical speed, centrifugal motion is observed in Ship-lap, Osborn, and Step liners. As a result, centrifugal motion can be eliminated in the Lorain liner by increasing the mill rotation speed. On the contrary, in the Step liner, the centrifugal motion of the mill disappears as the mill speed decreases. At 70% of critical speed, the highest head height is 306.47 cm for the Rib liner. the highest shoulder height is 247.13 cm for the Wave liner, also, the maximum impact zone length is 49.59 cm for the Step liner. But at 80% of critical speed, the highest head height is 313.54 cm for Rib and Lorain liners and the highest charge shoulder height is 251.66 cm for the Osborn liner. Also, the maximum impact zone length is 52.32 cm for the Osborn liner. By comparing the values of head height and shoulder height, it can be concluded that the shoulder height does not follow a certain rule, so it cannot be used as an appropriate criterion for evaluating the impact mechanism and comminution performance of the mill. For this reason, head height has been replaced as an evaluation criterion and is used in

this study as a suitable criterion. At 70% and 80% of critical speed, the lowest toe height, belonging to the Lorain liner, is 33.60 and 35.32 cm, respectively. As can be seen, the toe height values do not follow a specific rule, so the toe height cannot be used as an appropriate criterion for evaluating mill performance. Consequently, in this study, the impact zone length has been selected and replaced as another suitable criterion for the evaluation of mill performance. In this study, contrary to previous works, in which shoulder and toe heights were considered as the basis for investigating the impact mechanism and mill performance, for the first time, charge head height and impact zone length are considered as the main criteria for evaluating impact mechanism and mill performance. Therefore, the values for these two parameters are shown in capital letters in Table 5.

Fig. 6(a) shows the effect of mill shell liner type on charge head height at 70% of critical speed. As can be seen, the highest head height is related to the Rib liner. As a result, cataract motions and impact mechanisms are more prominent in this liner, which improves mill performance. The obvious difference is due to the proper number and thickness of the liner lifters. The charge head height of other liners is also significantly higher than the Smooth liner. Figure 6(b) demonstrates the effect of mill shell liner type on the impact zone length at 70% of critical speed. According to the diagram, the Wave Liner has a shorter impact zone length than the Smooth liner and has a negative effect on the impact zone length, impact mechanism, and mill performance. But other liners increase the impact zone length than the Smooth liner. Also, the most positive effect is related to Step liner. Figure 6(c) illustrates the effect of mill shell liner type on the charge head height at 80% of critical speed. It is observed that Rib, Lorain, and Osborn liners provide the highest charge head height, while Ship-lap and Step liners provide relatively good height, but the Wave liner raises the charging head slightly to the Smooth liner. Figure 6(d) demonstrates the effect of mill shell liner type on the impact zone length at 80% of critical speed. In this part of the figure, the impact zone length on the Wave and Lorain liners is reduced compared to the Smooth liner. As a result, these liners have had an adverse effect on the impact mechanism on the mill. It can be said that in areas of the industry where a higher abrasion mechanism is required, Wave liner is recommended at 80% of critical speed. Other liners increase the impact zone length, also the best performance is related to Osborn and Rib liners.

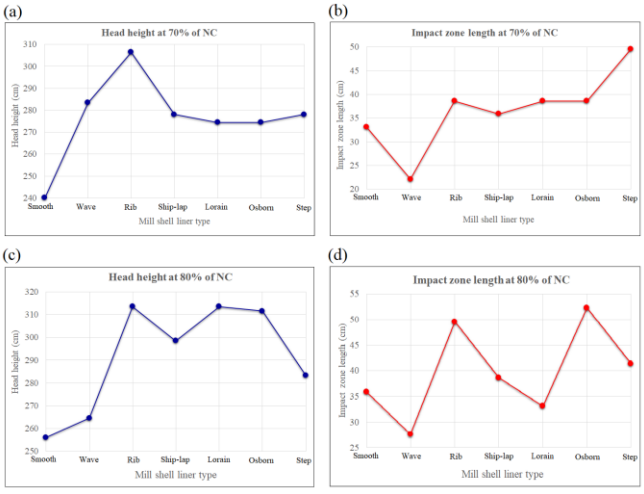

Figure 6. Effect of mill shell liner types on charge (a) head height at 70% of N_C; (b) impact zone length at 70% of N_C; (c) head height at 80% of N_C; (d) impact zone length at 80% of N_C.

Figure 7(a) demonstrates the effect of mill rotation speed on charge head height for different types of mill shell liners. According to the diagram, increasing the mill speed in all cases except the Wave liner increases the charge head height and thereby improves the impact mechanism in them. But in the Wave liner, this reduces the impact mechanism and increases the abrasion mechanism. The most positive effect of speed increase is related to Rib, Lorain, and Osborn liners.

Figure 7(b) illustrates the effect of increasing mill speed on impact zone length for different types of mill shell liners. Here, it can be seen that the increase in speed again has a favorable effect on increasing the impact zone length on all liners except for the Step and Lorain ones. The most positive effect is related to Osborn and Rib liners.

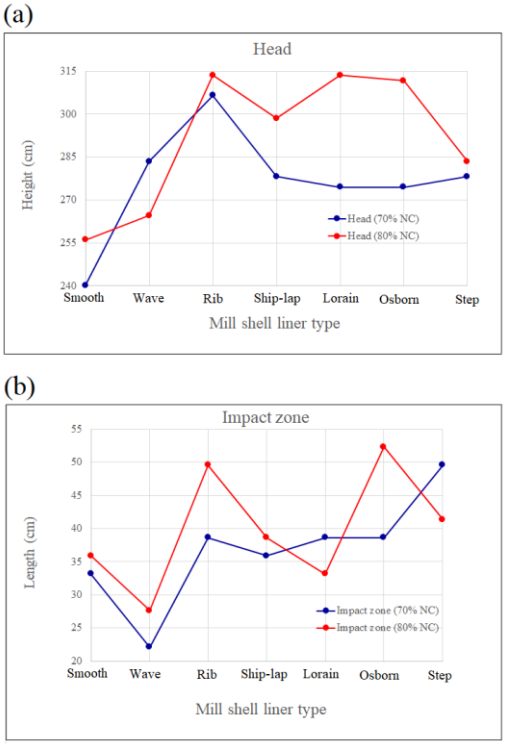

Figure 7. Effect of mill rotation speed on charge (a) head height; (b) impact zone length for different mill shell liner types.

Figure 8 illustrates the effect of mill rotation speed on charge head heights and impact zone lengths for different types of mill shell liners simultaneously. According to the figure, Smooth, Wave, and Step liners are not suitable for impact mechanisms due to reduced head height or impact zone length and are recommended for industries that require abrasion mechanisms. But Ship-Lap and Lorain liners only increase head height while to have a negligible or even undesirable effect on impact zone length, so these liners are not recommended for impact mechanism and further research should be done to optimize their performance. On the other hand, Osborn and Rib liners increase both head height and impact zone length, so they are suggested as suitable liners for the impact mechanism in this study. Meanwhile, the Osborn liner, due to its geometric shape, causes a large number of balls to be trapped in its lifters, which not participating in such a large number of balls in the comminution process will make the mill energy not usefully used for comminution. In general, according to all conditions, Rib liner is introduced as the optimal liner for impact mechanism in this research. It is worth noting that none of the liners used in this study are optimized and optimization of each of them separately is the subject of future author research.

Figure 9 shows the effect of different types of mill shell liners on the change of charge head height (a) and impact zone length (b) compared to Smooth liner at 70% and 80% of critical speed. As can be seen, the greatest effect of mill speed change on charge head height is related to Osborn, Wave, and Lorain Liners, respectively. Also, the least effect of mill speed change on the charge head height is related to the Ship-lap liner. On the other hand, changing the mill speed has the greatest effect on the impact zone length of the Osborn, Step, Lorain, and Rib liners and has no effect on the impact zone length of the Ship-lap liner. In general, the effect of mill speed change on the performance of the Lorian and Osborn liners is maximal and the performance of the Ship-lap liner is minimal.

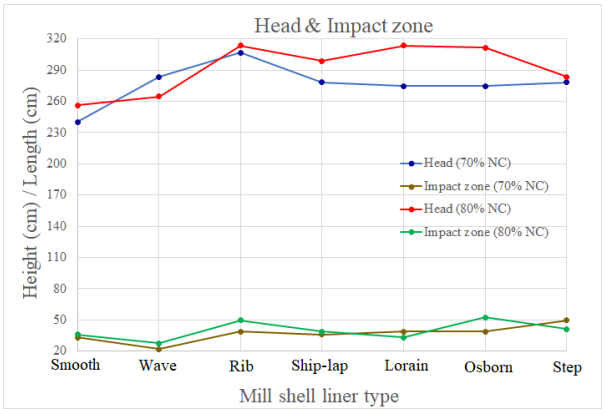

Figure 8. Effect of mill rotation speed on charge head heights and impact zone lengths for different mill shell liner types.

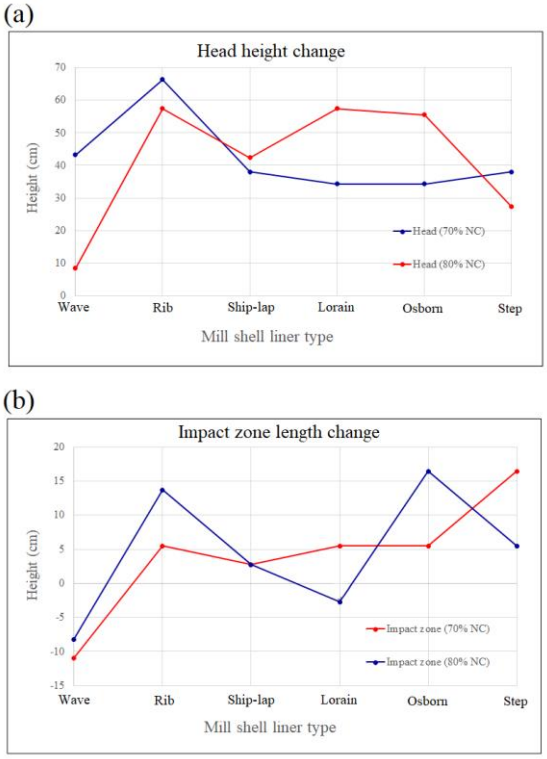

Figure 9. Effect of different mill shell liner types on change of (a) charge head height and (b) impact zone length in comparison to the Smooth liner at 70% and 80% of critical speed.

4.1. Validation

Since the DEM approach offers such strong advantages in modeling and understanding the milling process, both DEM simulations and the DEM solver must be validated properly and adequately. In general, a comprehensive validation of DEM solver and simulations is not feasible and, in most cases, it can be done only partially. In order to ensure the integrity of the application of the DEM techniques to comminution technology and other possible areas, the quality of validation should be improved and directed at the outputs being used in the modeling [52].

In this work, in order to validate the simulation results, a laboratory-scale SAG mill is simulated (Fig. 10) because it is easier to photograph due to its lower depth. Also, head, shoulder, toe, and impact points are more easily recognizable than ball mills. The laboratory-scale SAG mill is according to the dimensions described in Bian et al. [24]. The detailed geometrical and operational conditions and material properties for the laboratory-scale SAG mill are listed in Tables 6 – 8, respectively.

To validate the obtained results and also the LIGGGHTS DEM solver, charge head height and impact zone length of simulations conducted by this software for the laboratory scale SAG mill are compared with charge head height and impact zone length of experimental results under similar conditions (Figs. 11–13 and Table 9). The high agreement between the results indicates their validity and also the validity of the DEM solver.

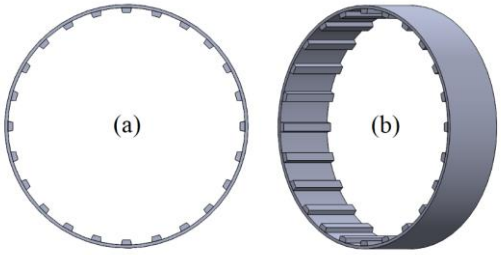

Figure 10. Laboratory scale SAG mill (a) 2D geometry; (b) 3D geometry.

Table 6- Laboratory scale SAG mill dimensions and speeds [24].

Laboratory scale SAG mill	Dimensions
Shell thickness (cm)	0.75
Mill length (cm)	16
Mill diameter (cm)	57.3
Mill volume (cm^3)	41259
N_C (Critical speed) (rpm)	56.88
Rotation speed (60% of N_C) (rpm)	32.79
Rotation speed (70% of N_C) (rpm)	38.26
Rotation speed (75% of N_C) (rpm)	40.99
Rotation speed (80% of N_C) (rpm)	43.72
Rotation speed (90% of N_C) (rpm)	49.19
The direction of rotation of the mill	Clockwise
Trapezoid lifter length (cm)	16
Trapezoid lifter thickness (cm)	1.20
Trapezoid lifter widths (cm)	1.95 and 2.45

Table 7- DEM ball Size distribution and numbers [24].

Ball size class (mm)	Number of balls	Mass fraction (%)
20	111	5.68
15	795	17.16
13	3051	42.87
8	10474	34.29
Total	14331	100

Table 8- Parameters used for the DEM simulations of the laboratory scale SAG mill [24].

DEM model details	Value
% Fill of ball charge	40
The total mass of ball charge (kg)	62.8734
DEM spring constant (kg/m)	10^6
Ball density (kg/m^3)	7800
Ball sliding friction coefficient	0.5
Ball rolling friction coefficient	0.01
Poisons ratio	0.25
Young's modulus (N/m^2)	1×10^9
Ball restitution coefficient	0.5

Table 9- comparison of the charge head height (cm) and impact zone length (cm) of simulations of the laboratory scale SAG mill using LIGGGHTS DEM solver and real pictures of experimental results [24] at the same operating conditions.

Simulations of the laboratory scale SAG mill				Real pictures of experimental results			
Mill rotation speed (rpm)	Mill rotation speed (%)	Head height (cm)	Impact zone length (cm)	Mill rotation speed (rpm)	Mill rotation speed (%)	Head height (cm)	Impact zone length (cm)
32.79	60% of N_C	51.23	4.50	32.79	60% of N_C	50.92	4.99
38.26	70% of N_C	52.68	7.97	38.26	70% of N_C	52.68	7.48
40.99	75% of N_C	54.18	9.46	40.99	75% of N_C	55.57	7.97
43.72	80% of N_C	55.90	12.40	43.72	80% of N_C	56.57	11.91
49.19	90% of N_C	56.95	15.79	49.19	90% of N_C	57.14	18.18

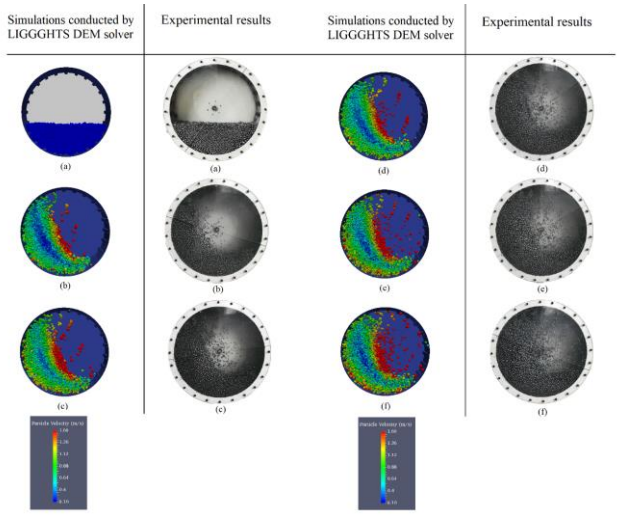

Figure 11. Comparison between simulations of the laboratory scale SAG mill using LIGGGHTS DEM solver and experimental results [24] at the same operating conditions when the drum is rotating at (a) 0% of N_C; (b) 60% of N_C; (c) 70% of N_C; (d) 75% of N_C; (e) 80% of N_C; and (f) 90% of N_C.

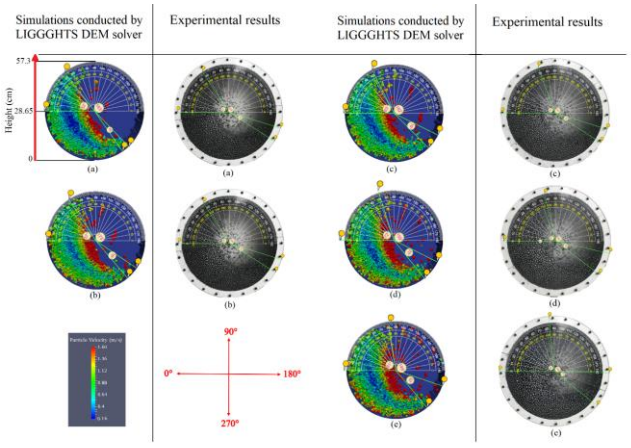

Figure 12. Using an online protractor to determine and compare the charge head height (cm) and impact zone length (cm) of simulations of the laboratory scale SAG mill using LIGGGHTS DEM solver and real pictures of experimental results at the same operating conditions when the drum is rotating at (a) 0% of N_C; (b) 60% of N_C; (c) 70% of N_C; (d) 75% of N_C; (e) 80% of N_C; and (f) 90% of N_C.

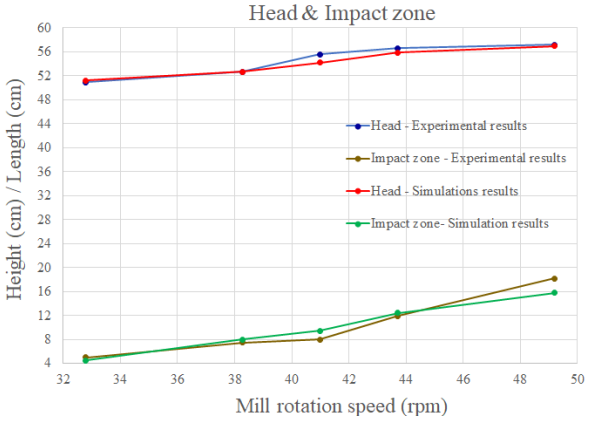

Figure 13. Validation of simulation results of the laboratory scale SAG mill by comparison with experimental results at the same operating conditions at different mill rotation speeds (rpm).

5. Conclusion

In this research, an open-source software LIGGGHTS was used to perform DEM simulations for industrial-scale ball mills with seven different liner types i.e. Smooth, Wave, Rib, Ship-lap, Lorain, Osborn, and Step liners. Following results were obtained:

- In Smooth, Wave, and Step liners, due to their appearance, the head height was not created properly and the balls slid over each other. As a result, the abrasion mechanism on these liners was more than other liners.
- In edged and angled liners such as Rib, Ship-lap, Lorain, and Osborn the appropriate head height was created.
- In the Lorain liner, with 6 thick lifters, the proper head height was provided, but because of the low number of lifters, the impact zone length was not created properly.
- In the Rib liner, with 12 low-thickness lifters, due to enough number of lifters, both head height and impact zone length was properly created.
- In the Osborn liner, with 60 low-thickness lifters, due to the equal distance between the lifters and the diameter of the selected balls (6 cm) in this study, a significant percentage of the balls stuck to the mill wall and caused centrifugal motion, so most of the balls were not participate in the comminution mechanism.
- Increasing the mill rotation speed by 10% did not have a significant effect on the impact mechanism improvement in most mills. It significantly increased the charge head height on the Lorain and Osborn liners but did not eliminate the problem of the low or high number of lifters in them.
- According to Figures 3 and 4, as well as research conducted and ongoing by the authors of this paper, the optimum number of lifters for ball mills was between 8 and 32 lifters with a medium thickness.
- Wave, Rib, and Ship-lap liners had an appropriate number of lifters but the number of Lorain liner lifters was less than optimal. Therefore, it was suggested to improve its performance dramatically by increasing the number of lifters to 8 to 12 (due to their high thickness).
- In the Osborn liner, because of the excessive number of lifters, it was suggested to reduce the number of lifters to 16 to 32 (due to their low thickness) to improve the performance of the liner.
- In the Ship-lap and Step liners, by increasing the acute angle and removing the corners in their lifters, the balls could be prevented from adhering to the mill wall.
- There was a cascade motion in all the liners.
- There was no cataracting motion in the Smooth liner.
- Only in the Wave liner, with the increase of the mill speed, the cataract motion disappeared, indicating that it had an adverse effect on its performance.
- At 70% of critical speed, a centrifugal motion was observed in Ship-lap, Lorain, and Osborn liners, which was much more dramatic in the Osborn liner for the above-mentioned reasons.
- At 80% of critical speed, the centrifugal motion was observed in Ship-lap, Osborn, and Step liners. As a result, the centrifugal motion could be eliminated in the Lorain liner by increasing the mill rotation speed. On the contrary, in the Step liner, the centrifugal motion of the mill disappeared as the mill speed decreases.
- By comparing the values of head height and shoulder height, it could be concluded that the shoulder height did not follow a certain rule, so it could not be used as an appropriate criterion for evaluating the impact mechanism and comminution performance of the mill. For this reason, head height was replaced as an evaluation criterion and used in this study as a suitable criterion.
- The toe height values did not follow a specific rule, so the toe height could not be used as an appropriate criterion for evaluating mill performance as well. Consequently, in this study, the impact zone length was selected and replaced as another suitable criterion

for the evaluation of mill performance.

- In this study, contrary to previous works, in which shoulder and toe heights were considered as the basis for investigating the impact mechanism and mill performance, for the first time, charge 'head height' and 'impact zone length' were introduced and considered as the main criteria for evaluating impact mechanism and mill performance.
- At 70% of critical speed, the highest head height was related to the Rib liner. As a result, cataract motions and impact mechanisms were more prominent in this liner, which improved mill performance. The obvious difference was due to the proper number and thickness of the liner lifters.
- At 70% of critical speed, the Wave Liner had a shorter impact zone length than the Smooth liner and had a negative effect on the impact zone length, impact mechanism, and mill performance. But other liners increased the impact zone length than the Smooth liner and the most positive effect was related to the Step liner.
- At 80% of critical speed, Rib, Lorain, and Osborn liners provided the highest charge head height, while Ship-lap and Step liners provided relatively good height, but the Wave liner raised the charging head slightly to the Smooth liner.
- At 80% of critical speed, the impact zone length on the Wave and Lorain liners was reduced compared to the Smooth liner. As a result, these liners had an adverse effect on the impact mechanism on the mill. Other liners increased the impact zone length, also the best performance was related to Osborn and Rib liners.
- In areas of the industry where a higher abrasion mechanism is required, Wave liner is recommended.
- Increasing the mill speed in all cases except the Wave liner increased the charge head height and thereby improved the impact mechanism in them. But in the Wave liner, this reduced the impact mechanism and increases the abrasion mechanism.
- The most positive effect of speed increase was related to Rib, Lorain, and Osborn liners.
- Increasing the mill speed had a favorable effect on increasing the impact zone length on all liners except for the Step and Lorain ones. The most positive effect was related to Osborn and Rib liners.
- Smooth, Wave, and Step liners were not suitable for impact mechanism due to reduced head height or impact zone length and were recommended for industries that require abrasion mechanism.
- Ship-Lap and Lorain liners only increased head height while had a negligible or even undesirable effect on impact zone length, so these liners were not recommended for impact mechanism and further research should be done to optimize their performance.
- Osborn and Rib liners increased both head height and impact zone length, so they were suggested as suitable liners for the impact mechanism in this study.
- The Osborn liner, due to its geometric shape, caused a large number of balls to be trapped in its lifters, which not participating in such a large number of balls in the comminution process made the mill energy not usefully used for comminution.
- In general, according to all conditions, Rib liner was introduced as the optimal liner for impact mechanism in this research.
- It is worth noting that none of the liners used in this study were optimized and optimization of each of them separately is the subject of future author research.
- The greatest effect of mill speed change on charge head height was related to Osborn, Wave, and Lorain Liners, respectively.
- The least effect of mill speed change on the charge head height was related to the Ship-lap liner.
- Changing the mill speed had the greatest effect on the impact zone length of the Osborn, Step, Lorain, and Rib liners and had no effect on the impact zone length of the Ship-lap liner.
- In general, the effect of mill speed change on the performance of the Lorian and Osborn liners was maximal and the performance of the Ship-lap liner was minimal.
- To validate simulation results, a laboratory-scale SAG mill was simulated. Comparison of the simulations related to the laboratory scale SAG mill with experimental results demonstrated a good agreement which validated the DEM simulations and the software used.
- The results indicated that the charge heads were respectively about 240.13, 283.40, 306.47, 278.12, 274.42, 274.42, and 278.12 cm at the simulations performed with Smooth, Wave, Rib, Ship-lap, Lorain, Osborn, and Step liners at 70% of NC. The corresponding values at 80% of NC were as follows: 256.08, 264.56, 313.54, 298.45, 313.54, 311.60, and 283.40 cm.
- On the other hand, the impact zone lengths were respectively about 33.14, 22.11, 38.63, 35.86, 38.63, 38.63, and 49.59 cm at the simulations performed with the above-mentioned liners at 70% of NC. The corresponding values for impact zone lengths at 80% of NC were as follows: 35.86, 27.63, 49.59, 38.63, 33.14, 52.32, and 41.38 cm.

Acknowledgments

The authors thank Shahrood University of Technology and Professor Mohammad Ataei for providing the supercomputer required for DEM simulations.

REFERENCES

[1] G. Rosales-Marín, J. Andrade, G. Alvarado, J.A. Delgadillo, E.T. Tuzcu, "Study of lifter wear and breakage rates for different lifter geometries in tumbling mill: Experimental and simulation analysis using population balance model", Minerals Engineering, 141, September 2019.

[2] B. K. Mishra and R. K. Rajamani, "The discrete element method for the simulation of ball mills", Appl. Math. Modelling, 16, 598 – 604, 1992.

[3] M.S. Powell, A.T. McBride, "A three-dimensional analysis of media motion and grinding regions in mills", Minerals Engineering, 17, 1099–1109, 2004.

[4] P.W. Cleary, "Predicting charge motion, power draw, segregation and wear in ball mills using discrete element methods", Minerals Engineering, 11, 1061-1080, 1998.

[5] P. W. Cleary, "Charge behaviour and power consumption in ball mills: sensitivity to mill operating conditions, liner geometry and charge composition", Int. J. Miner. Process. 63, 79–114, 2001.

[6] J. T. Kalala, M. M. Bwalya, M. H. Moys, "Discrete element method (DEM) modelling of evolving mill liner profiles due to wear. Part I: DEM validation", Minerals Engineering 18,1386–1391, 2005.

[7] J. T. Kalala, M. Bwalya, M.H. Moys, "Discrete element method (DEM) modelling of evolving mill liner profiles due to wear. Part II. Industrial case study", Minerals Engineering, 18, 1392–1397, 2005.

[8] S. Banisi, M. Hadizadeh, "3-D liner wear profile measurement and analysis in industrial SAG mills", Minerals Engineering, 20, 132–139, 2007.

[9] M. Yahyaei, S. Banisi, M. Hadizadeh, "Modification of SAG mill liner shape based on 3-D liner wear profile measurements", Int. J. Miner. Process. 91, 111–115, 2009.

[10] P. W. Cleary, "Recent Advances in DEM modelling of tumbling mills", Minerals Engineering, 14, 1295 – 1319, 2001.

[11] M. K. Abd El-Rahman, B. K. Mishra, R. K. Rajamani, "Industrial tumbling mill power prediction using the discrete element method", Minerals Engineering, 14, 1321–1328, 2001.

[12] P. W. Cleary, R. Morrisson, S. Morrell, "Comparison of DEM and experiment for a scale model SAG mill", Int. J. Miner. Process., 68,129– 165, 2003.

[13] B. K. Mishra, "A review of computer simulation of tumbling mills by the discrete element method Part II—Practical applications", Int. J. Miner. Process., 71, 95– 112, 2003.

[14] R. D. Morrison, P. W. Cleary, "Using DEM to model ore breakage within a pilot-scale SAG mill", Minerals Engineering 17, 1117–1124, 2004.

[15] N. Djordjevic, F. N. Shi, R. Morrison, "Determination of lifter design, speed and filling effects in AG mills by 3D DEM", Minerals Engineering, 17, 1135–1142, 2004.

[16] N. Djordjevic, R. Morrison, B. Loveday, P. Cleary, "Modelling comminution patterns within a pilot-scale AG/SAG mill", Minerals Engineering, 19, 1505–1516, 2006.

[17] M. Maleki-Moghaddam, A. R. Ghasemi, M. Yahyaei, S. Banisi, "The impact of the end-wall effect on the charge trajectory in tumbling model mills", Int. J. Miner. Process., 144, 75 – 80, 2015.

[18] P. Owen, P. W. Cleary, "The relationship between charge shape characteristics and fill level and lifter height for a SAG mill", Minerals Engineering, 83, 19–32, 2015.

[19] N. S. Weerasekara, L. X. Liu, M. S. Powell, "Estimating energy in grinding using DEM modelling", Minerals Engineering, 85, 23–33, 2016.

[20] P. W. Cleary, P. Owen, "Development of models relating charge shape and power draw to SAG mill operating parameters and their use in devising mill operating strategies to account for liner wear", Minerals Engineering, 117, 42–62, 2018.

[21] L. Xu, K. Luo, Y. Zhao, "Numerical prediction of wear in SAG mills based on DEM simulations", Powder Technology, 329, 353–363, 2018.

[22] P. W. Cleary, P. Owen, "Effect of operating condition changes on the collisional environment in a SAG mill", Minerals Engineering, 132, 297–315, 2019.

[23] A. R. Hasankhoei, M. Maleki-Moghaddam, A. Haji-Zadeh, M. E. Barzgar, S. Banisi, "On dry SAG mills end liners: Physical modeling, DEM-based characterization and industrial outcomes of a new design", Minerals Engineering, 141, 105835, 2019.

[24] X. Bian, G. Wang, H. Wang, S. Wang, W. Lv, "Effect of lifters and mill speed on particle behaviour, torque, and power consumption of a tumbling ball mill: Experimental study and DEM simulation", Minerals Engineering, Minerals Engineering,105, 22 – 35, 2017.

[25] F. Pedrayes, J. G. Norniella, M. G. Melero, J. M. Menéndez-Aguado, J. J. Juan J. del Coz-Díaz, "Frequency domain characterization of torque in tumbling ball mills using DEM modelling: Application to filling level monitoring", Powder Technology, 323, 433 – 444, 2018.

[26] B. A. Wills, T.J., Napier-Munn, "Wills' Mineral Processing Technology", 8th edition. Elsevier, pp. 147–180. Chapter 7, 2016.

[27] P. W. Cleary, "Large scale industrial DEM modeling", Eng. Comput. 21,169–204, 2004.

[28] P. W. Cleary, M. D. Sinnott, R. D. Morrison, "DEM prediction of particle flows in grinding processes", Int. J. Numer. Methods Fluids 58, 319–353, 2008.

[29] P. W. Cleary, "Ball motion, axial segregation and power consumption in a full scale two chamber cement mill", Miner. Eng. 22, 809–820, 2009.

[30] J. Kozicki, F. V. Donzé, "YADE-OPEN DEM: an open-source software using a discrete element method to simulate granular material", Eng. Comput. 26, 786–805, 2009.

[31] J. Chen, B. Huang, F. Chen, X. Shu, "Application of discrete element method to Superpave gyratory compaction", Road Mater. Pavement 13, 480–500, 2012.

[32] L. Zhang, S.F. Quigley, A. H. C. Chan, "A fast scalable implementation of the two-dimensional triangular Discrete Element Method on a GPU platform", Adv. Eng. Softw. 60–61, 70–80, 2013.

[33] H. Kruggel-Emden, M. Sturm, S. Wirtz, V. Scherer, "Selection of an appropriate time integration scheme for the discrete element method (DEM)", Comput. Chem. Eng. 32, 2263–2279, 2008.

[34] B. Nassauer, T. Liedke, M. Kuna, "Polyhedral particles for the discrete element method Geometry representation, contact detection, and particle generation", Granul. Matter, 15, 85–93, 2013.

[35] A. O. Raji, J. F. Favier, "Model for the deformation in agricultural and food particulate materials under bulk compressive loading using discrete element method. I: theory, model development, and validation", J. Food Eng. 64, 359–371, 2004.

[36] B. Nassauer, M. Kuna, "Contact forces of polyhedral particles in discrete element method", Granul. Matter, 15, 349–355, 2013.

[37] R. Balevičius, A. Džiugys, R. Kačianauskas, A. Maknickas, K. Vislavičius, "Investigation of performance of programming approaches and languages used for numerical simulation of granular material by the discrete element method", Comput. Phys. Commun. 175, 404–415, 2006.

[38] G. W. Delaney, P. W. Cleary, R. D. Morrison, S. Cummins, B. Loveday, "Predicting breakage and the evolution of rock size and shape distributions in Ag and SAG mills using DEM", Miner. Eng. 50–51, 32–139, 2013.

[39] J. M. Ting, M. Khwaja, L. R. Meachum, J. D. Rowell, "An ellipse-based discrete element model for granular materials", Int. J. Numer. Anal. Methods Geomech. 17, 603–623, 1993.

[40] I. Shmulevich, "State of the art modeling of soil–tillage interaction using discrete element method", Soil Tillage Res. 111, 41–53, 2010.

[41] P. W. Cleary, M. L. Sawley, "DEM modelling of industrial granular flows: 3D case studies and the effect of particle shape on hopper discharge, Appl. Math. Model. 26, 89–111, 2002.

[42] P. W. Cleary, "Industrial particle flow modelling using discrete element method, Eng. Comput. 26, 698–743, 2009.

[43] P. W. Cleary, M. D. Sinnott, "Assessing mixing characteristics of particle-mixing and granulation devices, Particuology, 6, 419–444, 2008.

[44] P. W. Cleary, "DEM prediction of industrial and geophysical particle flows", Particuology, 8, 106–118, 2010.

[45] P. W. Cleary, R. D. Morrison, "Particle methods for modelling in mineral processing", Int. J. Comput. Fluid Dyn. 23,137–146, 2009.

[46] S. Just, G. Toschkoff, A. Funke, D. Djuric, G. Scharrer, J. Khinast, K. Knop, P. Kleinebudde, "Experimental analysis of tablet properties for discrete element modeling of an active coating process", AAPS PharmSciTech 14, 402–411, 2013.

[47] W. McBride, P. W. Cleary, "An investigation and optimization of the 'OLDS' elevator using Discrete Element Modeling", Powder Technol. 193, 216–234, 2009.

[48] C. Goniva, C. Kloss, N.G. Deen, J.A.M. Kuipers, S. Pirker, "Influence of rolling friction on single spout fluidized bed simulation,

Particuology 10, 582–591, 2012.

[49] C. Goniva, C. Kloss, A. Hager, S. Pirker, "An open-source CFD–DEM perspective", Proceedings of OpenFOAM Workshop Gothenburg, Sweden, 2010.

[50] C. Kloss, C. Goniva, G. Aichinger, S. Pirker, "Comprehensive DEM–DPM–CFD simulations—model synthesis, experimental validation and scalability", Seventh International Conference on CFD in the Minerals and Process Industries CSIRO, Melbourne, Australia, 2009.

[51] B. A. Wills, "Wills' Mineral Processing Technology – An Introduction to the Practical Aspects of Ore Treatment and Mineral Recovery", Eighth Edition, Butterworth-Heinemann, Elsevier, 2016.

[52] N.S. Weerasekara, M.S. Powell, P. W. Cleary, L.M. Tavares, M. Evertsson, R.D. Morrison, J. Quist, R.M. Carvalho, "The contribution of DEM to the science of comminution", Powder Technol. 248 (2013) 3–24..